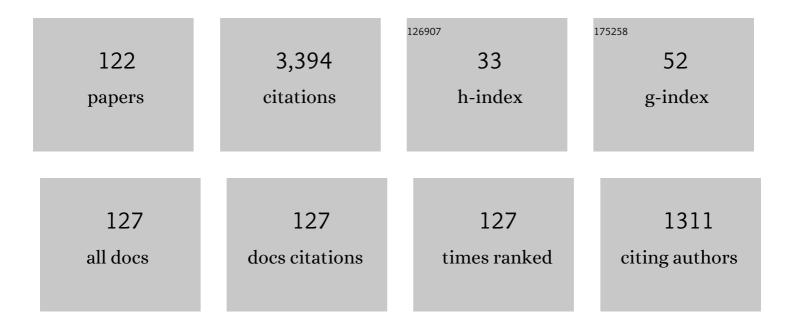
Li-Juan Chen

List of Publications by Year in descending order

Source: https://exaly.com/author-pdf/427964/publications.pdf Version: 2024-02-01



#	Article	IF	CITATIONS
1	Hydroxyl-and-carboxyl ligand concatenating multi-lanthanide substituted tellurotungstates and electrochemical detection of noradrenaline. Journal of Rare Earths, 2022, 40, 1785-1793.	4.8	3
2	An unprecedented dumbbell-shaped pentadeca-nuclear W-Er heterometal cluster stabilizing nanoscale hexameric arsenotungstate aggregate and electrochemical sensing properties of its conductive hybrid film-modified electrode. Nano Research, 2022, 15, 3628-3637.	10.4	40
3	Dual-heteroatom-templated lanthanoid-inserted heteropolyoxotungstates simultaneously comprising Dawson and Keggin subunits and their composite film applied for electrochemical immunosensing of auximone. Inorganic Chemistry Frontiers, 2022, 9, 350-362.	6.0	15
4	Double Trigonal Pyramidal {SeO3} Groups Bridged 2-Picolinic Acid Modified Cerium-Inlaid Polyoxometalate Including Mixed Selenotungstate Subunits for Electrochemically Sensing Ochratoxin A. Inorganic Chemistry, 2022, 61, 1949-1960.	4.0	7
5	Two Innovative Fumaric Acid Bridging Lanthanide-Encapsulated Hexameric Selenotungstates Containing Mixed Building Units and Electrochemical Performance for Detecting Mycotoxin. Inorganic Chemistry, 2022, 61, 10965-10976.	4.0	5
6	Multi-Nuclear Rare-Earth-Implanted Tartaric Acid-Functionalized Selenotungstates and Their Fluorescent and Magnetic Properties. Inorganic Chemistry, 2021, 60, 2533-2541.	4.0	17
7	Multicomponent Selfâ€Assembly of a Giant Heterometallic Polyoxotungstate Supercluster with Antitumor Activity. Angewandte Chemie - International Edition, 2021, 60, 11153-11157.	13.8	145
8	Tricarboxylic-Ligand-Decorated Lanthanoid-Inserted Heteropolyoxometalates Built by Mixed-Heteroatom-Directing Polyoxotungstate Units: Syntheses, Structures, and Electrochemical Sensing for 17Î2-Estradiol. Inorganic Chemistry, 2021, 60, 7536-7544.	4.0	19
9	Hexameric to Trimeric Lanthanide-Included Selenotungstates and Their 2D Honeycomb Organic–Inorganic Hybrid Films Used for Detecting Ochratoxin A. ACS Applied Materials & Interfaces, 2021, 13, 35997-36010.	8.0	35
10	Alkali metal–lanthanide co-encapsulated 19-tungsto-2-selenate derivative and its electrochemical detection of uric acid. Inorganic Chemistry Communication, 2021, 130, 108734.	3.9	1
11	Nicotinic-Acid-Ornamented Tetrameric Rare-Earth-Substituted Phospho(III)tungstates with the Coexistence of Mixed Keggin/Dawson Building Blocks and Its Honeycomb Nanofilm for Detecting Toxins. Inorganic Chemistry, 2021, 60, 14457-14466.	4.0	10
12	3-D Antimonotungstate Framework Based on 2,6-H ₂ pdca-connecting Iron–Cerium Heterometallic Krebs-type Polyoxotungstates for Detecting Small Biomolecules. Inorganic Chemistry, 2021, 60, 2663-2671.	4.0	15
13	{HPO ₃ } and {WO ₄ } Simultaneously Induce the Assembly of Tri-Ln(III)-Incorporated Antimonotungstates and Their Photoluminescence Behaviors. Inorganic Chemistry, 2021, 60, 1037-1044.	4.0	22
14	Three Lanthanide-Functionalized Antimonotungstate Clusters with a {Sb ₄ O ₄ Ln ₃ (H ₂ O) ₈ } Core: Syntheses, Structures, and Properties. Inorganic Chemistry, 2021, 60, 18065-18074.	4.0	13
15	Lanthanide-Incorporated Borotungstates Including Keggin-type [BW ₁₁ O ₃₉] ^{9â€"} Fragments and Their Luminescence Properties. Crystal Growth and Design, 2020, 20, 362-369.	3.0	11
16	A terbium-antimony-oxo-cluster bridging antimonotungstate comprising divacant and tetravacant Keggin segments. Inorganic Chemistry Communication, 2020, 111, 107625.	3.9	1
17	Double-Oxalate-Bridging Tetralanthanide Containing Divacant Lindqvist Isopolytungstates with an Energy Transfer Mechanism and Luminous Color Adjustablility Through Eu ³⁺ /Tb ³⁺ Codoping. Inorganic Chemistry, 2020, 59, 648-660.	4.0	44
18	First series of mixed (P ^{III} , Se ^{IV})-heteroatomoriented rare-earth-embedded polyoxotungstates containing distinct building blocks. Inorganic Chemistry Frontiers, 2020, 7, 4640-4651.	6.0	23

#	Article	IF	CITATIONS
19	Organic–Inorganic Hybrid Cerium-Encapsulated Selenotungstate Including Three Building Blocks and Its Electrochemical Detection of Dopamine and Paracetamol. Inorganic Chemistry, 2020, 59, 15355-15364.	4.0	30
20	A trimeric tri-Tb ³⁺ including antimonotungstate and its Eu ³⁺ /Tb ³⁺ /Dy ³⁺ /Gd ³⁺ -codoped species with luminescence properties. Dalton Transactions, 2020, 49, 12401-12410.	3.3	7
21	A Pentaâ€Eu ^{III} Sandwiched Dawson Selenotungstate and Its Unique Luminescence Properties. European Journal of Inorganic Chemistry, 2020, 2020, 3416-3425.	2.0	6
22	Organic–Inorganic Two-Dimensional Hybrid Networks Constructed from Pyridine-4-Carboxylate-Decorated Organotin–Lanthanide Heterometallic Antimotungstates. Inorganic Chemistry, 2020, 59, 11287-11297.	4.0	12
23	Construction of Ln ³⁺ -Substituted Arsenotungstates Modified by 2,5-Thiophenedicarboxylic Acid and Application in Selective Fluorescence Detection of Ba ²⁺ in Aqueous Solution. Inorganic Chemistry, 2020, 59, 6839-6848.	4.0	25
24	Multi-praseodymium-and-tungsten bridging octameric tellurotungstate and its 2D honeycomb composite film for detecting estrogen. Nanoscale, 2020, 12, 10842-10853.	5.6	28
25	An unprecedented polyhydroxycarboxylic acid ligand bridged multi-Eu ^{III} incorporated tellurotungstate and its luminescence properties. Dalton Transactions, 2020, 49, 8933-8948.	3.3	24
26	Two unusual nanosized Nd ³⁺ -substituted selenotungstate aggregates simultaneously comprising lacunary Keggin and Dawson polyoxotungstate segments. Nanoscale, 2020, 12, 16091-16101.	5.6	26
27	Acetate-Decorated Tri-Ln(III)-Containing Antimonotungstates with a Tetrahedral {WO ₄ } Group as a Structure-Directing Template and Their Luminescence Properties. Inorganic Chemistry, 2020, 59, 3954-3963.	4.0	30
28	Polyoxometalate-based composite materials in electrochemistry: state-of-the-art progress and future outlook. Nanoscale, 2020, 12, 5705-5718.	5.6	118
29	Preparations, Structures and Luminescence Properties of Pentaâ€rareâ€earth Incorporated Tetravacant Dawson Selenotungstates and Their Ho ³⁺ /Tm ³⁺ Coâ€doped Derivatives. Chemistry - an Asian Journal, 2020, 15, 1156-1166.	3.3	9
30	A novel 1-D chain organic–inorganic hybrid Cull–PrIII heterometallic germanomolybdate decorated by 2-picolinic acid ligands. Inorganic Chemistry Communication, 2020, 113, 107764.	3.9	2
31	Rare-Earth and Antimony-Oxo Clusters Simultaneously Connecting Antimonotungstates Comprising Divacant and Tetravacant Keggin Fragments. Inorganic Chemistry, 2019, 58, 11636-11648.	4.0	33
32	2-Picolinate-Decorated Iron–Lanthanide Heterometallic Germanotungstates Including an S-Shaped [Ge ₂ W ₂₀ O ₇₂] ^{16–} Segment. Inorganic Chemistry, 2019, 58, 15853-15863.	4.0	12
33	A novel inorganic–organic hybrid 3d–4f heterometallic germanotungstate based on saturated Keggin-type [α-GeW12O40]4â^' polyanion. Inorganic Chemistry Communication, 2019, 108, 107542.	3.9	5
34	Two Ce ³⁺ -Substituted Selenotungstates Regulated by <i>N</i> , <i>N</i> -Dimethylethanolamine and Dimethylamine Hydrochloride. Inorganic Chemistry, 2019, 58, 8442-8450.	4.0	37
35	Two Penta-RE ^{III} Encapsulated Tetravacant Dawson Selenotungstates and Nanoscale Derivatives and Their Luminescence Properties. Inorganic Chemistry, 2019, 58, 7078-7090.	4.0	25
36	Two 1,3-bis[tris(hydroxymethyl)methylamino]propane functionalized 3d–4f heterometallic arsenotungstates. Inorganic Chemistry Communication, 2019, 105, 63-68.	3.9	1

#	Article	IF	CITATIONS
37	Three Types of Distinguishing <scp>l</scp> -Alanine-Decorated and Rare-Earth-Incorporated Arsenotungstate Hybrids Prepared in a Facile One-Step Assembly Strategy. Inorganic Chemistry, 2019, 58, 3479-3491.	4.0	32
38	Organic–inorganic hybrid 1-D double chain heteropolymolybdates constructed from plenary Keggin germanomolybdate anions and hepta-nuclear Cu–RE–pic heterometallic clusters. Dalton Transactions, 2019, 48, 15977-15988.	3.3	15
39	A 1-D chain transition-metal substituted germanomolybdate constructed from di-Cull-substituted sandwich-type heteropolyoxomolybdate units linked by doubly di-Nal-cluster bridges. Inorganic Chemistry Communication, 2019, 99, 119-125.	3.9	1
40	Aggregation of Giant Cerium–Bismuth Tungstate Clusters into a 3D Porous Framework with High Proton Conductivity. Angewandte Chemie - International Edition, 2018, 57, 8416-8420.	13.8	221
41	Three Types of Mixed Alkaliâ€Metalâ€, Transitionâ€Metalâ€, or Rareâ€Earthâ€Substituted Sandwichâ€Type Arsenotungstates with Supporting Rareâ€Earth Pendants. European Journal of Inorganic Chemistry, 2018, 2018, 143-152.	2.0	8
42	Frontispiz: Aggregation of Giant Cerium–Bismuth Tungstate Clusters into a 3D Porous Framework with High Proton Conductivity. Angewandte Chemie, 2018, 130, .	2.0	0
43	Frontispiece: Aggregation of Giant Cerium–Bismuth Tungstate Clusters into a 3D Porous Framework with High Proton Conductivity. Angewandte Chemie - International Edition, 2018, 57, .	13.8	1
44	Synergistic Effect between Different Coordination Geometries of Lanthanides and Various Coordination Modes of 2-Picolinic Acid Ligands Tuning Three Types of Rare 3d–4f Heterometallic Tungstoantimonates. Inorganic Chemistry, 2018, 57, 15079-15092.	4.0	50
45	First Dimethyltin-Functionalized Rare-Earth Incorporated Tellurotungstates Consisting of {B·Î±-TeW ₇ O ₂₈ } and {W ₅ O ₁₈ } Mixed Building Units. Inorganic Chemistry, 2018, 57, 12509-12520.	4.0	30
46	Ligandâ€Controlled Assembly of Heteropolyoxomolybdates from Plenary Keggin Germanomolybdates and Cu–Ln Heterometallic Units. Chemistry - an Asian Journal, 2018, 13, 3762-3775.	3.3	13
47	Unprecedented Selenium and Lanthanide Simultaneously Bridging Selenotungstate Aggregates Stabilized by Four Tetraâ€vacant Dawsonâ€like {Se ₂ W ₁₄ } Units. Chemistry - an Asian Journal, 2018, 13, 2897-2907.	3.3	16
48	Aggregation of Giant Cerium–Bismuth Tungstate Clusters into a 3D Porous Framework with High Proton Conductivity. Angewandte Chemie, 2018, 130, 8552-8556.	2.0	30
49	Recent advances in isopolyoxotungstates and their derivatives. Acta Crystallographica Section C, Structural Chemistry, 2018, 74, 1202-1221.	0.5	11
50	Syntheses, structures and fluorescence properties of three rare-earth containing docosatungstates. Spectrochimica Acta - Part A: Molecular and Biomolecular Spectroscopy, 2017, 176, 114-122.	3.9	13
51	Syntheses, structural characterization and photophysical properties of two series of rare-earth-isonicotinic-acid containing Waugh-type manganomolybdates. CrystEngComm, 2017, 19, 834-852.	2.6	15
52	Coexistence of long-range ferromagnetic ordering and spin-glass behavior observed in the first inorganic–organic hybrid 1-D oxalate-bridging nona-Mn ^{II} sandwiched tungstoantimonate chain. Journal of Materials Chemistry C, 2017, 5, 2043-2055.	5.5	37
53	Syntheses, structural characterization and electrochemical properties of two rare-earth–isonicotinic-acid containing silicomolybdates. Inorganic Chemistry Communication, 2017, 83, 1-6.	3.9	5
54	Organocounterions-Assisted and pH-Controlled Self-Assembly of Five Nanoscale High-Nuclear Lanthanide Substituted Heteropolytungstates. Crystal Growth and Design, 2017, 17, 3917-3928.	3.0	29

#	Article	IF	CITATIONS
55	Structural Transformation from Dimerization to Tetramerization of Serineâ€Decorated Rareâ€Earthâ€Incorporated Arsenotungstates Induced by the Usage of Rareâ€Earth Salts. Chemistry - A European Journal, 2017, 23, 2673-2689.	3.3	95
56	Rare-Earth-Incorporated Tellurotungstate Hybrids Functionalized by 2-Picolinic Acid Ligands: Syntheses, Structures, and Properties. Inorganic Chemistry, 2017, 56, 13228-13240.	4.0	35
57	Syntheses, structural characterization and photoluminescence properties of {AsO 2 (OH)}-bridging arsenotungstates incorporating lanthanide ions. Journal of Solid State Chemistry, 2017, 256, 196-202.	2.9	2
58	Tellurotungstate-Based Organotin–Rare-Earth Heterometallic Hybrids with Four Organic Components. Inorganic Chemistry, 2017, 56, 7257-7269.	4.0	53
59	Two Families of Rare-Earth-Substituted Dawson-type Monomeric and Dimeric Phosphotungstates Functionalized by Carboxylic Ligands. Crystal Growth and Design, 2017, 17, 5295-5308.	3.0	22
60	Lanthanide-Connecting and Lone-Electron-Pair Active Trigonal-Pyramidal-AsO3 Inducing Nanosized Poly(polyoxotungstate) Aggregates and Their Anticancer Activities. Scientific Reports, 2016, 6, 26406.	3.3	37
61	Trigonal Pyramidal {AsO ₂ (OH)} Bridging Tetranuclear Rare-Earth Encapsulated Polyoxotungstate Aggregates. Inorganic Chemistry, 2016, 55, 3881-3893.	4.0	63
62	Syntheses, structures and properties of two copper-2-picolinic-acid germanomolybdate hybrids with mixed organic components. Inorganic Chemistry Communication, 2016, 71, 113-118.	3.9	5
63	First quadruple-glycine bridging mono-lanthanide-substituted borotungstate hybrids. Dalton Transactions, 2016, 45, 16471-16484.	3.3	23
64	Synthesis, structure and electrochemical properties of an inorganic–organic hybrid Cu II Ce III heterometallic germanotungstate. Inorganic Chemistry Communication, 2016, 71, 54-60.	3.9	7
65	Syntheses, structures and properties of a series of inorganic–organic hybrid copper–lanthanide heterometal comprising germanotungstates with mixed ligands. Synthetic Metals, 2016, 217, 256-265.	3.9	9
66	Hydrothermal syntheses, crystal structures and characterization of two new 1-D and 2-D inorganic–organic hybrid polyoxomolybdates [H 2 dap] 2 [x-Mo 8 O 26]·2H 2 O and [Cu(dap) 2] 2 [β-Mo 8 O 26]. Inorganic Chemistry Communication, 2016, 63, 24-29.	3.9	7
67	The main progress over the past decade and future outlook on high-nuclear transition-metal substituted polyoxotungstates: from synthetic strategies, structural features to functional properties. Dalton Transactions, 2016, 45, 4935-4960.	3.3	45
68	Research progress on polyoxometalate-based transition-metal–rare-earth heterometallic derived materials: synthetic strategies, structural overview and functional applications. Chemical Communications, 2016, 52, 4418-4445.	4.1	245
69	A brief review of the crucial progress on heterometallic polyoxotungstates in the past decade. CrystEngComm, 2016, 18, 842-862.	2.6	47
70	Self-Assembly of a Family of Isopolytungstates Induced by the Synergistic Effect of the Nature of Lanthanoids and the pH Variation in the Reaction Process: Syntheses, Structures, and Properties. Crystal Growth and Design, 2016, 16, 108-120.	3.0	24
71	Syntheses and Structures of Two Organic–Inorganic Composite Vanadoborates Na2(Hen)4[B18V12O60]·16H2O and (H2en)6[B18V12O60]2·2tepa·11H2O. Synthesis and Reactivity in Inorganic, Metal Organic, and Nano Metal Chemistry, 2016, 46, 687-693.	0.6	4
72	Two types of novel tetra-iron substituted sandwich-type arsenotungastates with supporting lanthanide pendants. Dalton Transactions, 2015, 44, 12598-12612.	3.3	46

#	Article	IF	CITATIONS
73	Synthesis, structure and properties of an organic–inorganic hybrid independent 1-D double-chain Keggin-type silicotungstate with mixed ligands. Inorganic Chemistry Communication, 2015, 54, 25-30.	3.9	8
74	The first purely inorganic polyoxotungstates constructed from dimeric tungstoantimonate-based iron–rare-earth heterometallic fragments. CrystEngComm, 2015, 17, 5002-5013.	2.6	32
75	A novel Dawson-like cerium(IV)-hybridizing selenotungstate Na13H7[Ce(SeW17O59)2]·31H2O. Inorganic Chemistry Communication, 2015, 56, 35-40.	3.9	19
76	Synthesis, Crystal Structure, and Magnetic Property of an Organic–Inorganic Hybrid Silicotungstate With Supporting Dinuclear Copper Complexes. Synthesis and Reactivity in Inorganic, Metal Organic, and Nano Metal Chemistry, 2015, 45, 682-687.	0.6	1
77	Significant developments in rare-earth-containing polyoxometalate chemistry: synthetic strategies, structural diversities and correlative properties. CrystEngComm, 2015, 17, 8175-8197.	2.6	77
78	Synthesis, structure and electrochemical properties of a Fe III –Ce III heterometallic sandwich-type tungstoantimonate with novel 2-D infinite structure [Ce(H 2 O) 8][Ce(H 2 O) 6][Fe 4 (H 2 O) 10 (B-β-SbW) Tj E	Tᡚ.øO00	rg B T /Overlc
79	Two Organic–Inorganic Hybrids Assembled from Transition–Metal Complexes and Keggin-Type Silicotungstates. Journal of Cluster Science, 2015, 26, 2005-2022.	3.3	0
80	Two octamolybdate-based hybrids functionalized by 1,3-bis[tris(hydroxymethyl)methylamino]propane ligand. Inorganic Chemistry Communication, 2015, 61, 68-72.	3.9	5
81	Synthesis, structure, spectroscopic and ferroelectric properties of an acentric polyoxotungstate containing 1:2-type [Sm(α-PW11O39)2]11┠fragment and d-proline components. Spectrochimica Acta - Part A: Molecular and Biomolecular Spectroscopy, 2015, 134, 101-108.	3.9	11
82	Syntheses, structures and properties of three metal–organic complexes containing 2,2′-dipyridyl-5,5′-dicarboxylate ligands. Journal of Solid State Chemistry, 2015, 221, 5-13.	2.9	7
83	Synthesis, Structure, and Properties of a 2-D Organic–Inorganic Hybrid Phosphotungstate-Based Cu ^{II} –La ^{III} Heterometallic Derivative. Synthesis and Reactivity in Inorganic, Metal Organic, and Nano Metal Chemistry, 2014, 44, 171-176.	0.6	1
84	Hydrothermal synthesis and structural characterization of an organic–inorganic hybrid sandwich-type tungstoantimonate [Cu(en)2(H2O)]4[Cu(en)2(H2O)2][Cu2Na4(α-SbW9O33)2]•6H2O. Journal of Solid State Chemistry, 2014, 209, 113-119.	2.9	8
85	Rectangle versus Square Oxalate-Connective Tetralanthanide Cluster Anchored in Lacunary Lindqvist Isopolytungstates: Syntheses, Structures, and Properties. Crystal Growth and Design, 2014, 14, 5495-5505.	3.0	35
86	Hydrothermal Synthesis and Structural Characterization of a 1-D Inorganic-Organic Composite Tetra-Nickel Substituted Sandwich-Type Phosphotungstate. Synthesis and Reactivity in Inorganic, Metal Organic, and Nano Metal Chemistry, 2014, 44, 118-124.	0.6	0
87	A 3-D framework based on mono-copper II substituted silicotungstate units [Cu(dap) 2 (H 2 O)] 2 [Cu(dap) 2][α-SiW 11 CuO 39]·2H 2 O. Inorganic Chemistry Communication, 2014, 50, 19-23.	3.9	4
88	First Tungstoantimonate-Based Transition-Metal–Lanthanide Heterometallic Hybrids Functionalized by Amino Acid Ligands. Crystal Growth and Design, 2014, 14, 6217-6229.	3.0	66
89	Syntheses, structures and electrochemical properties of a class of 1-D double chain polyoxotungstate hybrids [H ₂ dap][Cu(dap) ₂] _{0.5} [Cu(dap) ₂ (H ₂ O)][Ln(H< Dalton Transactions, 2014, 43, 5694-5706,	รนี้ชี>2 รเ</td <td>sup>(O<du></du></td>	sup>(O <du></du>
90	Recent progress in metal-functionalized germanotungstates: from structures to properties. RSC Advances, 2014, 4, 50679-50692.	3.6	13

#	Article	IF	CITATIONS
91	Novel One-Dimensional Organic–Inorganic Polyoxometalate Hybrids Constructed from Heteropolymolybdate Units and Copper–Aminoacid Complexes. Crystal Growth and Design, 2014, 14, 1467-1475.	3.0	45
92	Syntheses, structures, spectroscopic and electrochemical properties of two 1D organic–inorganic Cull–LnIII heterometallic germanotungstates. Spectrochimica Acta - Part A: Molecular and Biomolecular Spectroscopy, 2013, 114, 360-367.	3.9	14
93	A novel organic–inorganic hybrid sandwich-type germanotungstate with discrete [Fe4(en)2(α-GeW9O34)2]8â" polyoxoanions and 1-D [Fe4(en)(α-GeW9O34)2]n8nâ^ polymeric chains. Inorgani Chemistry Communication, 2013, 33, 99-104.	്ദ.9	11
94	Synthesis, characterization, magnetic and electrochemical properties of a new 3D hexa-copper-substituted germanotungstate. Journal of Solid State Chemistry, 2013, 205, 82-90.	2.9	4
95	Syntheses, structures and properties of three new two-dimensional Cul–LnIII heterometallic coordination polymers based on 2,2′-dipyridyl-5,5′-dicarboxylate ligands. Spectrochimica Acta - Part A: Molecular and Biomolecular Spectroscopy, 2013, 116, 348-354.	3.9	7
96	An organic–inorganic hybrid 1-D double-chain copper–yttrium heterometallic silicotungstate [Cu(dap)2(H2O)]2{Cu(dap)2[α-H2SiW11O39Y(H2O)2]2}•10H2O. Inorganic Chemistry Communication, 2013, 27, 13-17.	3.9	17
97	Tetrahedral Polyoxometalate Nanoclusters with Tetrameric Rare-Earth Cores and Germanotungstate Vertexes. Crystal Growth and Design, 2013, 13, 4368-4377.	3.0	38
98	Novel polyoxometalate hybrids consisting of copper–lanthanide heterometallic/lanthanide germanotungstate fragments. Dalton Transactions, 2012, 41, 10740.	3.3	71
99	2-D and 3-D phosphotungstate-based TM–Ln heterometallic derivatives constructed from dimeric [Ln(α-PW11O39)2]11Ⱐfragments and copper-organic complex linkers. Journal of Solid State Chemistry, 2012, 196, 29-39.	2.9	24
100	A six-connected 3-D framework [enH2]2[Cu(en)2]3[H2W12O42]·6H2O constructed from paratungstate-based polyoxometalate units. Inorganic Chemistry Communication, 2012, 25, 35-38.	3.9	8
101	Novel 1-D double-chain organic–inorganic hybrid polyoxotungstates constructed from dimeric copper–lanthanide heterometallic silicotungstate units. CrystEngComm, 2012, 14, 7981.	2.6	38
102	A 2-D Organic–Inorganic Hybrid Copper-Yttrium Heterometallic Monovacant Keggin Phosphotungstate Derivative: [Cu(dap)2]5.5[Y(l±-PW11O39)2]·4H2O. Synthesis and Reactivity in Inorganic, Metal Organic, and Nano Metal Chemistry, 2012, 42, 30-36.	0.6	11
103	Three novel 2D organic–inorganic hybrid Cull–LnIII heterometallic arsenotungstates. Synthetic Metals, 2012, 162, 1030-1036.	3.9	12
104	Four types of 1D or 2D organic–inorganic hybrids assembled by arsenotungstates and Cull–LnIII/IV heterometals. CrystEngComm, 2012, 14, 3108.	2.6	58
105	Three 3D organic–inorganic hybrid heterometallic polyoxotungstates assembled from 1:2-type [Ln(α-SiW11O39)2]13⒠silicotungstates and [Cu(dap)2]2+ linkers. Synthetic Metals, 2012, 162, 1558-1565.	3.9	21
106	A novel organic–inorganic hybrid 3D framework based on neodymium oxalate–selenites [Nd2(SeO3)2(C2O4)(H2O)2]·2H2O. Synthetic Metals, 2012, 162, 1648-1653.	3.9	4
107	Two organic–inorganic hybrid 1-D and 3-D polyoxotungstates constructed from hexa-Cull substituted sandwich-type arsenotungstate units. CrystEngComm, 2012, 14, 2797.	2.6	52
108	An organic–inorganic hybrid hexa-nickel substituted sandwich-type germanotungstate [enH2]2[Ni(en)2]2{[Ni6(en)2(H2O)2][B-α-GeW9O34]2} 14H2O. Inorganic Chemistry Communication, 2012, 17, 79-83.	3.9	14

#	Article	IF	CITATIONS
109	Synthesis, structure and properties of a metal–organic complex built up from ferrous sulfate chains and 2,2'-bipyridyl-5,5'-dicarboxylic acid ligands. Inorganic Chemistry Communication, 2012, 20, 277-281.	3.9	11
110	Three Transition-Metal Substituted Polyoxotungstates Containing Keggin Fragments: From Trimer to One-Dimensional Chain to Two-Dimensional Sheet. Crystal Growth and Design, 2011, 11, 1913-1923.	3.0	68
111	Two 1-D multi-nickel substituted arsenotungstate aggregates. CrystEngComm, 2011, 13, 3462.	2.6	51
112	Two 3d–4f heterometallic monovacant Keggin phosphotungstate derivatives. Journal of Coordination Chemistry, 2011, 64, 400-412.	2.2	24
113	Synthesis, structure and magnetism of a S-shaped multi-iron substituted arsenotungstate containing a trivacant Keggin [B-î±-AsVW9O34]9â^' and a hexavacant Keggin [î±-AsVW6O26]11â^' fragments. Journal of Solid State Chemistry, 2011, 184, 2756-2761.	2.9	20
114	Two novel 2D organic–inorganic hybrid lacunary Keggin phosphotungstate 3d–4f heterometallic derivatives: [Cu(en)2]2H6[Ce(α-PW11O39)2]·8H2O and [Cu(dap)2(H2O)][Cu(dap)2]4.5[Dy(α-PW11O39)2]Â Inorganic Chemistry Communication, 2011, 14, 324-329.	à. 4H 20.	50
115	Synthesis, structure and magnetism of a 2-D organic–inorganic hybrid tetra-Coll-substituted sandwich-type Keggin germanotungstate: {[Co(dap)2(H2O)]2[Co(dap)2]2[Co4(Hdap)2(B-α-HGeW9O34)2]}·7H2O. Inorganic Chemistry Communication. 2011. 14. 1052-1056.	3.9	28
116	An organic–inorganic hybrid dimeric arsenotungstate [enH2]4{[Cu(en)2][(A-β-H2AsW9O34)Cu(en)2]2}·8H2O established by two trivacant Keggin [A-β-AsW9O34]9Ⱂ fragments in the opposite orientation. Inorganic Chemistry Communication, 2011, 14, 1178-1182.	3.9	14
117	An organic–inorganic hybrid nickel-substituted arsenotungstate consisting of three types of polyoxotungstate units. Inorganic Chemistry Communication, 2010, 13, 50-53.	3.9	26
118	One-pot syntheses, structures and properties of two novel 1-D copper complexes: [CuII2(Hbpdc)2CI2]2·2H2O and CuI(H2bpdc)Cl (H2bpdc = 2,2′-bipyridyl-5,5′-dicarboxylic acid). Inorganic Chemistry Communication, 2010, 13, 822-827.	3.9	30
119	Hydrothermal syntheses and structural characterization of two sandwich-type arsenotungstates. Journal of Coordination Chemistry, 2010, 63, 2042-2055.	2.2	12
120	A CdSO4-like 3-D framework constructed from monosodium substituted Keggin arsenotungstates and copper(II)-ethylenediamine complexes. Inorganic Chemistry Communication, 2009, 12, 707-710.	3.9	22
121	A Series of Inorganicâ^'Organic Hybrid Composite Solids Based on Molybdenum Oxide Chains. Crystal Growth and Design, 2006, 6, 2076-2085.	3.0	71
122	Organic–inorganic hybrid phosphite-participating S-shaped penta-CeIII incorporated tellurotungstate as electrochemical enzymatic hydrogen peroxide for β-D-glucose detection. Inorganic Chemistry Frontiers, 0, , .	6.0	7